Analysis and Validation of the Effect of Various Queueing Configurations to the End-to-End Throughput of Multi-Hop Wireless Network

Peng Hou Ho[1], Kim Chuan Lim[1], Kae Hsiang Kwong [2]
[1]Faculty of Electronic and Computer Engineering,
Universiti Teknikal Malaysia Melaka, Malaysia.
[2]Recovision Sdn. Bhd
1, Jalan Putra Mahkota 7/8D, Putra Point Business Centre,
Putra Heights, 47650 Subang Jaya, Selangor, Malaysia.
vshy108@gmail.com

Abstract—**A multi-hop wireless network is created by connecting multiple wireless access points (APs) as the backhaul of the network to increase the network coverage. The issue of spatial bias, unbalanced network performance of end-to-end throughput and delay occurs when the total offered load of the associated stations to the backhaul exceeds the wireless link capacity. Station associated to the access point with more hops away from the gateway will experience a significant amount of delay and lower end-to-end throughput compared to the station with fewer hops to the gateway. The equality of local successful transmit probability and mesh successful transmit probability in congested APs, which is the main root cause of the spatial bias problem, is modelled and validated. If the packet arrival ratio of local over mesh ingress interface is larger than the respective queue length ratio, the mesh ingress interface successful transmit probability will be higher than the local ingress interface successful transmit probability and vice-versa. By controlling the ratio of queue lengths, stations associated to the access point with more hops away from the gateway are given higher transmit opportunity, and therefore the spatial bias problem in multi-hop wireless network can be alleviated.**

Index Terms— **Multi-hop wireless network, spatial bias, access point, queueing discipline, queue length ratio, packet arrival ratio.**

I. INTRODUCTION

Nowadays, Wi-Fi service is available everywhere to provide internet connection for users. Wi-Fi service is a wireless connection provided by a device that adopts IEEE 802.11 standard defined by Wi-Fi Alliance. To extend the coverage of IEEE 802.11 wireless network with only one gateway, a multi-hop wireless network designed by relaying multiple access points (APs) in a chain topology can be deployed. An example of a 6-hop wireless network is shown in Figure 1.

Wireless Mesh Network (WMN) implementation such as open80211s [1] introduces the capabilities of self-healing, self-organizing and self-configuring to the backhaul of a
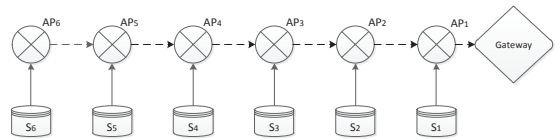

Figure 1: 6-hop wireless network (chain topology)

multi-hop wireless network. APs equipped with the functionality of WMN, also known as Mesh Access Points (MAPs), can provide connection between the non-mesh stations (station S_n, legacy wireless local area network stations) and the mesh network formed by the MAPs and Mesh Portal (MPP). The traffic produced by the associated non-mesh station is always received by the local ingress interface of a MAP for further packet forwarding (e.g. traffic produced by station S_n to MAP_n). The mesh traffic produced by a MAP is always forwarded to the mesh ingress interface of the target MAP (e.g. traffic of MAP_5 consists of traffic produced by S_6 and MAP_6, to MAP_4).

Whenever one of the MAPs (or more than one MAP) is congested (the total ingress traffics, from both the local and mesh ingress interfaces, exceeded the egress link capacity), the end-to-end throughput of the traffic belong to non-mesh station that is associated to fewer hops MAP outperforms the non-mesh node associated to more hops MAP (*e.g.* S_3 has better end-to-end throughput compared to S_5 when AP_4 is congested).

A transmit buffer (queue of waiting packets) is commonly allocated to the egress interface to fully utilize the wireless link capacity. The process of enqueueing packets into the transmit buffer is handled by a queueing manager (First-In-First-Out is the default queueing discipline used by the Linux queueing manager). The equality of the local successful transmit probability (a_n) and the mesh successful transmit probability (b_n) in congested MAPs introduced by the default queueing manager is the main root cause of the unbalanced

To demonstrate the existence of the problem as shown in Figure 2, a 6-hop wireless network testbed was formed with a multiple open80211s MAPs and a MPP. In the testbed, each of the MAPs was equipped with two wireless radio cards and one Ethernet card. IEEE 802.11g mode was configured for wireless communication. Interconnection medium between the wireless radio cards was provided by radio frequency (RF) coaxial cables (minimum interference, collision, propagation loss and almost zero error where the relationship between queueing disciplines and unbalanced end-to-end throughput problem can be focused to perform measurements and analysis). Non-overlapping channels were assigned to the network interfaces so that there was no co-channel interference and no adjacent channel interference caused by nearby access points.
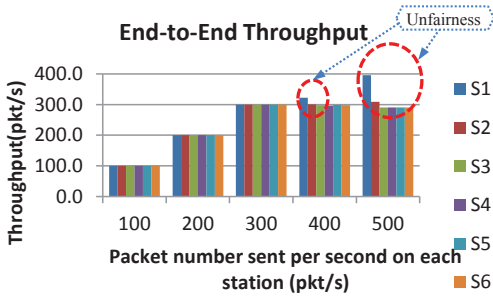

Figure 2: End-to-end Throughput with Different Offered Loads Produced by each of the Station

Distributed Internet Traffic Generator (D-ITG) version 2.8.0-rc1[2] was used to generate deterministic traffic. An Ethernet connection was set up between client and corresponding MAP to ensure the arrival distribution of local client traffic to MAP was the same as the client's D-ITG inter-departure time distribution. The time interval between two successive points in time at which customers depart from the queue after service is completed is called an inter-departure time [3]. Hence, in this case, Ethernet traffic can be treated as a client wireless traffic that works in an ideal scenario. The D-ITG client was set to have a deterministic inter-departure time distribution. Packet size was fixed to 1470 bytes. The hardware specification of the testbed is as follows:

Table 1
Hardware Specification of the Testbed

	MAP/MPP	Station
Model	Dell Precision T3500	Dell Inspiron 1122
Processor	Intel Xeon W3530 (Quad Core, 2.80GHz)	AMD C-60 APU (Dual Core, 1000MHz)
RAM	6GB DDR3 SDRAM	2GB DDR3 SDRAM
Networking	Ethernet x1	Ethernet x1
	Wireless Adaptor x 2 (Transmitter): TP-LINK TL-WN722N (Receiver): D-Link DWA-547 Wireless link capacity (μ_{max}, between Transmitter and Receiver): 1824pkt/s	

The successful transmit probability of the local ingress interface accepted packets on MAP$_n$ to MAP$_{n-1}$ is equal to:

$$a_n = \frac{p_{direct_L} + p_{--_L}}{p_{direct_L} + p_{drop_L} + p_{++_L}}, \qquad (1)$$

where p_{direct_L} is the number of local ingress interface received packets that are directly transmitted in one second, p_{--_L} is the number of local ingress interface received packets that are dequeued from the local client queue in one second, p_{drop_L} is the number of local ingress interface received packets that are dropped from local client queue in one second and p_{++_L} is the number of local ingress interface received packets that are enqueued into local client queue in one second. The successful transmit probability shall be equal to 1 if all the received packets (p_{direct_L} and p_{++_L}) are successfully sent to the next hop without any drop ($p_{drop_L} = 0$). The same measure is applied to the mesh ingress interface.

$$b_n = \frac{p_{direct_M} + p_{--_M}}{p_{direct_M} + p_{drop_M} + p_{++_M}} \qquad (2)$$

By configuring the testbed with offered load from each station as $\lambda_s = 400$pkt/s, the aggregated offered load in MAP$_2$ would have exceeded the wireless link capacity ($5\lambda_s > \mu_{max}$) and hence, both the MAP$_2$ and MAP$_1$ are congested. The respective a_n and b_n values of both MAPs are measured and the difference between them are shown in a histogram as depicted in Figure 3. The differences between the successful transmit probabilities are always small (Normal distributed, zero centered for MAP$_1$. Two modes, major population centered at zero and the second population centered at 0.035 for MAP$_2$).

The structure of this paper is as follows. Various methods that had been proposed to improve the end-to-end delay and end-to-end throughput in multi-hop wireless networks and WMNs are briefly discussed and summarized in Section II. To solve the unbalanced end-to-end throughput problem, a model to determine the required local successful transmit probability (a_n) and mesh successful transmit probability (b_n) in congested MAPs for n-hop wireless network is firstly presented. The required a_n and b_n values to alleviate the unbalanced end-to-end throughput problem will be subsequently determined from the model. To implement the required successful transmit probabilities into the congested MAPs, two virtual queues (one for each ingress interface) with different queue length ratio are proposed. The results of the different queue length ratio, which will drop the packet according to the defined ratio when the MAP is congested by the respective configured offered load, are then analysed and presented. The results showing the unbalanced end-to-end throughput introduced by the default queueing discipline manager, which have been alleviated with the queue length ratio determined from the model, are presented at the end of the result section. The outcomes of this paper and the possible future works will be concluded and discussed at the end of this paper.
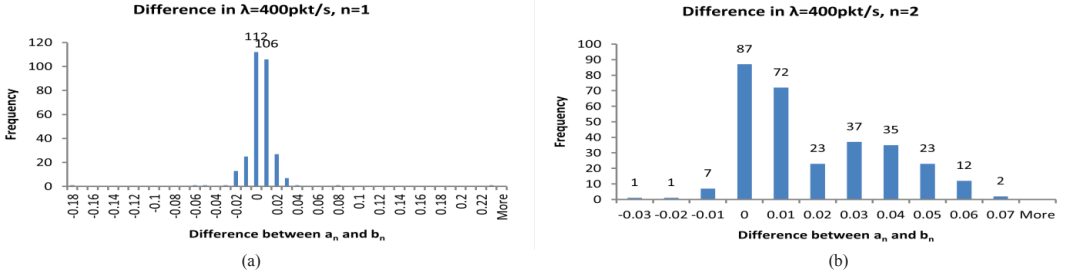
Figure 3: Histogram of the difference between a_n and b_n for $\lambda = 400\text{pkt}/s$ at (a) MAP$_1$ and (b) MAP$_2$.

II. RELATED WORKS

Various methods had been proposed to improve the end-to-end delay and end-to-end throughput in multi-hop wireless networks and WMNs. Bae *et al.* [4] determined a minimum contention window size based on Access Category (AC) of Enhanced Distribution Channel Access (EDCA) to support a fair end-to-end delay rather than the Distributed Coordination Function (DCF) regardless of nodes locations. Jung *et al.* [5] proposed to give a higher channel access probability to relay nodes with lower traffic forwarding capability by tuning the minimum contention window size of the binary exponential backoff (BEB) mechanism. Lopes Gomes *et al.* [6] proposed a fuzzy link cost (FLC) metric which is based on expected transmission count (ETX) and minimum delay (MD) link quality metrics to achieve Quality of Service (QoS) and Quality of Experience (QoE) requirements of WMN for multimedia packets.

Furthermore, Pinheiro *et al.* [7] proposed a Queue-based OLSR ETX (QoETX) approach by using a cross-layer scheme. Network and user-based parameters are optimized by coordinating queue availability, QoS and fuzzy issues in the routing decision process. System performance introduced by QoETX is improved because least congested routes in WMNs are selected based on the queue utilization. Another cross layer scheme was proposed by Fathi *et al.* [8], allowing scheduling scheme in Media Access Control/Physical layer (MAC/PHY) to cooperate with the rate-control mechanism in Transport layer, to improve the network performance in terms of end-to-end delay, aggregate utility, and fairness. Arrival rates at the base station are controlled by a rate-control mechanism and the departure rates from the nodes are determined in a joint channel-aware and queue-aware scheduling scheme.

Another method proposed by Nandiraju *et al.* [9], intended to achieve load balance among the available gateways by announcing the congestion status when the average queue utilization exceeded a limit. The active traffic sources can then switch to other better gateways to avoid congestion. Nandiraju *et al.* [10] also proposed Queue Management in Multi-Hop Networks (QMMN) algorithm that keeps updating fair share

value for each node by computing the average arrival rate and service time to achieve higher resource utilization with the aim of reducing spatial contention caused by increasing hop number. A modified version of the QMMN algorithm, Enhanced-QMMN (EQMMN) was implemented by Chilamkurti and Prakasam [11] to improve the Transmission Control Protocol (TCP) throughput and fairness index.

Lim et al. [12] proposed a weighted random early detection (wRED) mechanism that has a different dropping preference according to the hop-count information. The lesser is the dropping, the higher is the end-to-end throughput from the source node to the destination node. Similarly, Mancuso et al. [13] limited the single-hop nodes' rates to give more transmission opportunities to nodes that are more hops away.

III. THE DEFAULT FIFO QUEUE MANAGEMENT SYSTEM AND THE PROPOSED METHOD

The successful transmit probability of the respective network ingress interface with default FIFO queueing management system over *n*-hop is firstly modelled and presented in Section III.A. An example of making use of the derived model to determine the successful transmit probability of the local and mesh network ingress interface is presented at the end of the discussion. The equations to calculate the successful transmit probabilities of five different scenarios to be experienced by a MAP according to the parameters of the network (e.g. offered load, wireless link capacity and number of hops) are presented in Section III.B. The needed a_n and b_n values to equally divide the wireless link capacity among the connected MAPs in the testbed are also determined.

A. Default FIFO Queue Management System

A mathematical model describing the relationship between FIFO queueing and spatial bias problem in multi-hop wireless network introduced by the default FIFO queue management implemented in Linux based system, with restriction as discussed in Section III.A.1, is presented in this section.

1) FIFO Queue Management System Restrictions

Suppose a system is created under these restrictions:

I. All data packets have fixed packet size.

II. No loss besides dropped packet loss caused by full

queue condition in transmit queue.

III. Local client traffic arrives at MAP with the same rate in all hops and arrives in deterministic distribution, λ_s.

IV. Wireless uplink capacity of all wireless links has fixed value, μ_{max}. Congested network condition occurs in mesh network backhaul if

$$N\lambda_s > \mu_{max}, \quad (3)$$

where N is the total number of hops of the multi-hop network.

V. For a congested MAP, its transmit rate is equal to μ_{max}. Hence if MAP_C is the congested MAP that has the largest hop number, then MAPs that are fewer hops away than MAP_C to gateway (MAP_n which has hop number, $n < C$) should also be congested MAPs in this system.

A congested MAP is MAP_n that has a total of mesh traffic and local client traffic exceeding the wireless uplink capacity (similar with Gateway Airtime Saturation Property discussed by Mancuso *et al.* [13])

$$\lambda_{M_n} + \lambda_s > \mu_{max}, \quad (4)$$

where λ_{M_n} is the arrival rate on mesh ingress interface of MAP_n:

$$\lambda_{M_n} = \begin{cases} \mu_{max} & , if \ n < C \\ (N-n)\lambda_s & , if \ n \geq C \end{cases}, \quad (5)$$

where n is the hop number of MAP_n while C is the largest hop number for the congested MAPs. By substituting Eq. (5) into Eq. (4) for $n = C$,

$$(N-C)\lambda_s + \lambda_s > \mu_{max}, \quad (6)$$

From Eq. (6), the value of C can be determined as:

$$C < N + 1 - \frac{\mu_{max}}{\lambda_s}, C \in \mathbb{N}, \quad (7)$$

$$C = \begin{cases} N - \frac{\mu_{max}}{\lambda_s} & , if \ (N+1-\frac{\mu_{max}}{\lambda_s}) \in \mathbb{N} \\ \left\lfloor N+1-\frac{\mu_{max}}{\lambda_s} \right\rfloor & , if \ (N+1-\frac{\mu_{max}}{\lambda_s}) \notin \mathbb{N} \end{cases}, \quad (8)$$

$$C = \begin{cases} N - \frac{\mu_{max}}{\lambda_s} & , if \ \lambda_s | \mu_{max} \\ N+1+\left\lfloor -\frac{\mu_{max}}{\lambda_s} \right\rfloor & , if \ \lambda_s \nmid \mu_{max} \end{cases}, \quad (9)$$

$$C = \begin{cases} N - \frac{\mu_{max}}{\lambda_s} & , if \ \lambda_s | \mu_{max} \\ N+1-\left\lceil \frac{\mu_{max}}{\lambda_s} \right\rceil & , if \ \lambda_s \nmid \mu_{max} \end{cases}, \quad (10)$$

$$\because -\lfloor x \rfloor = \begin{cases} 1 - \lceil x \rceil & , if \ x \notin \mathbb{Z} \\ -\lceil x \rceil & , if \ x \in \mathbb{Z} \end{cases} \quad (11)$$

$$\therefore C = \begin{cases} N - \frac{\mu_{max}}{\lambda_s} & , if \ \lambda_s | \mu_{max} \\ N - \left\lceil \frac{\mu_{max}}{\lambda_s} \right\rceil & , if \ \lambda_s \nmid \mu_{max} \end{cases} \quad (12)$$

$$\because \frac{\mu_{max}}{\lambda_s} \in \mathbb{Z} \ if \ \lambda_s | \mu_{max} \quad (13)$$

$$\therefore \frac{\mu_{max}}{\lambda_s} = \left\lceil \frac{\mu_{max}}{\lambda_s} \right\rceil \ if \ \lambda_s | \mu_{max} \quad (14)$$

$$\therefore C = N - \left\lceil \frac{\mu_{max}}{\lambda_s} \right\rceil \quad (15)$$

where the floor function $\lfloor x \rfloor$ is the largest integer, but not greater than x, the ceiling function $\lceil x \rceil$ is the smallest integer, but not less than x, $x|y$ represents y is divisible by x and $x \nmid y$ represents y is not divisible by x. Congested network scenario is the prerequisite of having congested MAP and Eq. (3) can be rewritten as

$$\left(N + 1 - \frac{\mu_{max}}{\lambda_s}\right) > 1. \quad (16)$$

Example of multi-hop wireless system with the same local client traffic and wireless link capacity where congestion occurs at node MAP_C is shown in Figure 4.

2) Mathematical Modelling of Default FIFO System

For default FIFO queue management system, there is only a total queue length in the MAP_n transmission queue (Q_n) but it does not have any individual queue length for local ingress interface accepted packets (Q_{Ln}) and mesh ingress interface accepted packets (Q_{Mn}):

$$q_{Ln} + q_{Mn} \leq Q_n, \quad (17)$$

where q_{Ln} is the number of waiting packets in the transmission queue that were received by local ingress interface and q_{Mn} is the number of waiting packets in the transmission queue that were received by the mesh ingress interface.

In a congested MAP, the ratio of q_{Ln} to q_{Mn} is equal to the ratio of the arrival rate on the local ingress interface ($\forall \lambda_{L_n} = \lambda_s$) to the arrival rate on the mesh ingress interface (λ_{M_n}). Making use of the arrival rate of mesh ingress interface of MAP_n as defined in Eq. (5):

$$\frac{q_{Ln}}{q_{Mn}} = \frac{\lambda_{L_n}}{\lambda_{M_n}} = \frac{\lambda_s}{\lambda_{M_n}} = \begin{cases} \frac{\lambda_s}{\mu_{max}}, & if \ n < C \\ \frac{1}{(N-C)}, & if \ n = C \end{cases}. \quad (18)$$

Obviously, there is no waiting packet in a non-congested MAP because packets are always directly transmitted if no packet is waiting in the transmit queue:

$$q_{Ln} = q_{Mn} = 0, \quad if \ n > C. \quad (19)$$

Successful transmit rates to the next hop MAP (MAP_{n-1}) received by a specified ingress interface is equal to the product of arrival rate on the mesh ingress interface of the next hop MAP and the ratio of the arrival rate on the ingress interface to total arrival rate on the congested MAP:

$$\mu_{Ln} = \lambda_{M_{n-1}} \times \frac{\lambda_s}{\lambda_s + \lambda_{M_n}}, \quad (20)$$

$$\mu_{Mn} = \lambda_{M_{n-1}} \times \frac{\lambda_{M_n}}{\lambda_s + \lambda_{M_n}}, \quad (21)$$

where μ_{M_n} is the successful transmit rate to MAP_{n-1} for those packets received by mesh ingress interface in MAP_n and μ_{L_n} is the successful transmit rate to the MAP_{n-1} for those packets received by local ingress interface in MAP_n. The sum of all ingress interfaces successful transmit rate is equal to arrival rate on the mesh ingress interface at less one hop MAP:

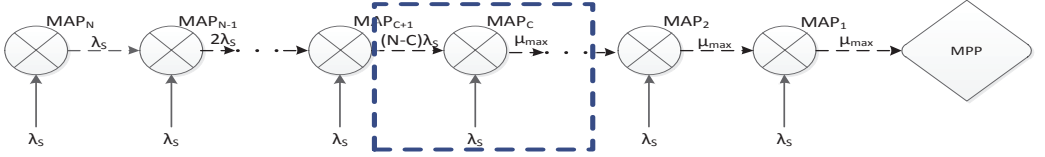$$\mu_{L_n} + \mu_{M_n} = \lambda_{M_{n-1}}. \quad (22)$$

Figure 4. Example of multi-hop wireless system where congestion occurs $((N-C)\lambda_s + \lambda_s > \mu_{max})$ at node MAP_C

Let a_n be the successful transmit probability of the local ingress interface accepted packets on MAP_n to MAP_{n-1}:

$$a_n = \frac{\mu_{L_n}}{\lambda_s} = \frac{\lambda_{M_{n-1}}}{\lambda_s + \lambda_{M_n}}. \qquad (23)$$

Let b_n be the successful transmit probability of the mesh ingress interface accepted packets on MAP_n to MAP_{n-1}:

$$b_n = \begin{cases} \frac{\mu_{M_n}}{\lambda_{M_n}} = \frac{\lambda_{M_{n-1}}}{\lambda_s + \lambda_{M_n}}, & n < N \\ \nexists, & n = N \end{cases}. \qquad (24)$$

The b_n does not exist when $n = N$ because $\lambda_{M_N} = 0$. By comparing Eq. (23) and Eq. (24), we have

$$a_n = b_n = \frac{\lambda_{M_{n-1}}}{\lambda_s + \lambda_{M_n}} \text{ when } n < N. \qquad (25)$$

By substituting Eq. (5) into Eq. (25), we have

$$a_n = b_n = \frac{\lambda_{M_{n-1}}}{\lambda_s + \lambda_{M_n}} =$$

$$\begin{cases} \frac{\mu_{max}}{\lambda_s + \mu_{max}} & , if\ n < C \\ \frac{\mu_{max}}{\lambda_s + (N-C)\lambda_s} = \frac{\mu_{max}}{(N-C+1)\lambda_s} & , if\ n = C \\ \frac{(N-(n-1))\lambda_s}{\lambda_s + (N-n)\lambda_s} = 1 & , if\ n > C \end{cases}. \qquad (26)$$

End-to-end throughput is denoted as λ_{n0} and it is equal to the number of packets transmitted from n-th hop station and successfully reaching MPP in one second:

$$\lambda_{n0} = a_n(\textstyle\prod_{i=1}^{n-1} b_i)\lambda_s. \qquad (27)$$

By substituting Eq. (26) into Eq. (27),

$$\lambda_{n0} = \begin{cases} \left(\frac{\mu_{max}}{\mu_{max}+\lambda_s}\right)^n \times \lambda_s & , if\ n < C \\ \frac{(\mu_{max})^C}{(N-C+1)(\mu_{max}+\lambda_s)^{C-1}} & , if\ n \geq C \end{cases}. \qquad (28)$$

3) An Example of Using Derived Model to Determine the value of a_n and b_n with Equal Deterministic Offered Load (400pkt/s) from Stations (n=6)

By substituting value of $\mu_{max} = 1824pkt/s$, $\lambda_s = 400pkt/s$, $N = 2$ and $C = 2$ into Eq.(26), the calculated successful transmit probabilities can be obtained:

$$a_n = b_n = \begin{cases} \frac{1824}{400+1824} = 0.82 & , if\ n < 2 \\ \frac{1824}{(6-2+1)400} = 0.91 & , if\ n = 2 \\ 1 & , if\ n > 2 \end{cases}. \qquad (29)$$

As what deduced in this Section III.A.3, the local successful transmit probability is inherently equal to the mesh successful transmit probability in multi-hop wireless network that uses the default FIFO.

B. Proposed Method to Determine the Required a_n and b_n Value for Equal End-to-End Throughput

The five possible scenarios to be experienced by the concatenation of MAP when the aggregated throughput exceeded the wireless link capacity is shown in Figure 5.

The value of C can be calculated by substituting $N = 6$, and wireless link capacity $\mu_{max} = 1824\ pkt/s$, with the offered load per station, λ_s, into Eq.(15):

$$C = N - \left\lfloor\frac{\mu_{max}}{\lambda_s}\right\rfloor = 2$$

$$\therefore 1 < C < N$$

End-to-end throughput (Eq. (27)):

$$\lambda_{n0} = a_n\left(\prod_{i=1}^{n-1} b_i\right)\lambda_s$$

Hence end-to-end throughput from n-th hop ($1 \leq n \leq N, N = 6$):

$$\lambda_{10} = a_1\lambda_s \qquad (30)$$
$$\lambda_{20} = a_2 b_1 \lambda_s \qquad (31)$$
$$\lambda_{30} = a_3 b_2 b_1 \lambda_s \qquad (32)$$
$$\lambda_{40} = a_4 b_3 b_2 b_1 \lambda_s \qquad (33)$$
$$\lambda_{50} = a_5 b_4 b_3 b_2 b_1 \lambda_s \qquad (34)$$
$$\lambda_{60} = a_6 b_5 b_4 b_3 b_2 b_1 \lambda_s \qquad (35)$$

Sum of all hop stations cannot exceed the wireless link capacity.

$$\sum_{n=1}^{N} \lambda_{n0} = \sum_{n=1}^{N} a_n\left(\prod_{i=1}^{n-1} b_i\right)\lambda_s \leq \mu_{max} \qquad (36)$$

Arrival rate of mesh ingress interface (λ_{M_n}) at MAP_n should be not more than the wireless link capacity:

$$\lambda_{M_n} = a_{n+1}\lambda_s + b_{n+1}\lambda_{M_{n+1}} \leq \mu_{max} \qquad (37)$$

When n is replaced with $(n-1)$,

$$\lambda_{M_{n-1}} = a_n\lambda_s + b_n\lambda_{M_n} \leq \mu_{max} \qquad (38)$$

In the mathematical model, all wireless link capacities in multi-hop wireless network are assumed to be equal to a constant value:
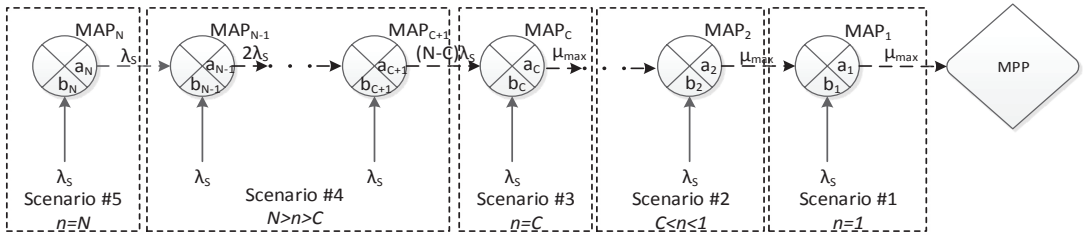
$$\forall \mu_{max_n} = \mu_{max} \qquad (39)$$

At MAP_N, arrival rate on mesh ingress interface is always equal to zero, hence the corresponding successful transmit probability, b_N is equal to do not care value, but it is assumed to be equal to zero in this system:

$$\lambda_{M_N} = 0, b_N = 0$$

and the successful transmit probability of the local ingress interface accepted packets at MAP_N is always equal to one when $N > C$,

$$a_N = 1$$

Figure 5: Four difference scenarios where MAP$_C$ is congested

All successful transmit probabilities that are deduced in the above formula is summarized in Table 2.

Table 2
Successful transmit probability values of multi-hop wireless network with $1 < C < N$

	$n = 1$	$1 < n < C$	$n = C$	$N > n > C$	$n = N$
a_n	$\frac{\lambda_{10}}{\lambda_s}$	$\frac{\lambda_{n0}}{(\prod_{i=1}^{n-1} b_i)\lambda_s}$	$\frac{\lambda_{C0}}{(\prod_{i=1}^{C-1} b_i)\lambda_s}$	1	1
b_n	$1 - \frac{\lambda_{10}}{\mu_{max}}$	$1 - \frac{a_n\lambda_s}{\mu_{max}}$	$\frac{\mu_{max} - a_C\lambda_s}{(N-C)\lambda_s}$	1	0
λ_{M_n}	μ_{max}	μ_{max}	$(N-C)\lambda_s$	$(N-n)\lambda_s$	0
λ_{L_n}	λ_s	λ_s	λ_s	λ_s	λ_s
μ_{max_n}	μ_{max}	μ_{max}	μ_{max}	μ_{max}	μ_{max}

In order to have equal end-to-end throughput (λ_{n0}), the wireless link capacity has to be equally divided by the number of MAP, hence,

$$\lambda_{n0} = \frac{\mu_{max}}{N} \quad (40)$$

The required a_n and b_n value for equal end-to-end throughput can then be determined by substituting Eq. (40) into Table 2 as shown in Table 3.

Table 3
Required a_n and b_n values for equal end-to-end throughput

	$n = 1$	$1 < n < C$	$n = C$	$N > n > C$	$n = N$
a_n	$\frac{\mu_{max}}{N\lambda_s}$	$\frac{\mu_{max}}{N(\prod_{i=1}^{n-1} b_i)\lambda_s}$	$\frac{\mu_{max}}{N(\prod_{i=1}^{C-1} b_i)\lambda_s}$	1	1
b_n	$1 - \frac{1}{N}$	$1 - \frac{a_n\lambda_s}{\mu_{max}}$	$\frac{\mu_{max} - a_C\lambda_s}{(N-C)\lambda_s}$	1	0

C. Hypothesis: The Ratio between the Length of Local and Mesh Ingress Interface Queue Can Affect the Successful Transmit Probability of the Respective Interface

When the sum of the arrival packet of local and mesh ingress interface exceeded the wireless link capacity, the packet will start queueing in the queue. Once the queue is full, additional arrival packet no matter arriving from local or mesh ingress interface will be dropped (not successfully transmitted). Only the packet remaining in the queue will be successfully transmitted to the next hop. Making use of the packet dropping design, if two queues are created (one for local and one for the mesh ingress interface) in such a way that the length of the queue will be filled up not according to the packet arrival ratio, the packet's successful transmit probability will be affected.

Provided the packet arrival ratio of MAP$_2$ as 1:4 (every single packet arrived at the local ingress interface, four packets would have arrived at the mesh ingress interface), if the queue length ratio is also 1:4 (*e.g.* 10 for local and 40 for mesh), whenever local ingress queue is full, the mesh ingress queue should also have filled up with packets. This queue length ratio will allow both the ingress interface to drop packet at the same rate (every time local ingress interface drops one packet, mesh ingress will drop one packet). A queue ratio of 1:5 (*e.g.* 10 for local and 50 for mesh) would allow mesh ingress interface to drop less packet compared to local ingress interface (whenever the local ingress queue already filled up with 10 packets, there will be 10 ($= 50 - 40$) packets space left in the mesh ingress interface, hence, increasing the successful transmit probability of the mesh ingress interface).

The results showing the validity of the hypothesis are presented in the next section.

IV. RESULTS AND DISCUSSION

Queueing configuration of the MAPs in the testbed is explained in Section IV.A. The obtained average end-to-end throughputs and the respective standard deviation of the proposed queue length configuration are presented in Section IV.B. The obtained successful transmit probability (a_1, b_1, a_2 and b_2) of the testbed with $1 < C < N$ ($C = 2$) under four different queueing configurations is also shown in Section IV.B. Discussion about the results is presented in Section IV.C.

A. Queueing Configuration of the MAPs in the Testbed

Multi-hop wireless network with local client traffic of 400pkt/s per station will congest the network. With the configured offered load of 400pkt/s per station, the node (MAP$_C$) where the aggregated traffic exceeded the wireless link capacity can be determined by Eq. (15) as follows:

$$C = N - \left\lfloor \frac{\mu_{max}}{\lambda_s} \right\rfloor = 6 - \left\lfloor \frac{1824}{400} \right\rfloor = 6 - 4 = 2$$

where $N = 6$, $\lambda_s = 400$pkt/s, and $\mu_{max} = 1824$ pkt/s (the measured wireless link capacity between the transmitter and receiver of the wireless adapter).

All the traffic in non-congested MAP (MAP$_n$, $n>C$) are assumed to have a complete successful transmit probability (a_n and b_n equal to one in direct transmission). Default FIFO configuration (single queue with length of 1000 packets, default Linux kernel 3.0.0rc2 configuration) is applied to the

non-congested MAPs ($n>C$) and abbreviated as Def. The queueing configuration of the testbed is summarized as shown in Table 4.

Table 4
Queueing configuration of the testbed
(N=6, C=2, $\lambda_s = 400$pkt/s, $\mu_{max} = 1824$ pkt/s)

	MAP6	MAP5	MAP4	MAP3	MAP2	MAP1
Scenario	n=N	C<n<N	C<n<N	C<n<N	n=C	n=1
Queueing configuration	Def	Def	Def	Def	To be configured with various queue length ratio	

B. Result

To validate the hypothesis in Section III.C, queues with different length ratios abbreviated as L*XX*_M*YY* (L for local and M for mesh, *e.g.* L10_M40 means the length of local ingress queue is 10 while the mesh ingress queue is 40 were configured in MAP1 and MAP2. (L100_M500 and L10_M50 were selected because comparison between L100_M500 and L10_M50 can show the effect of the total number of waiting packets on network performance with the same ratio value. Comparison between L10_M50 and L10_M40 can show the effect of slightly different ratio.)

The obtained average end-to-end throughputs and the respective standard deviation of the proposed queue length configuration (see Section IV.A) are shown in Figure 6.
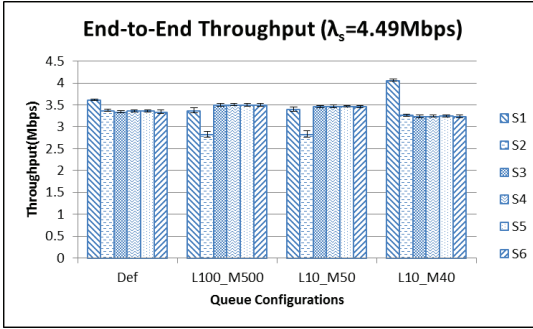

Figure 6: End-to-end throughput result with λ_s = 4.49Mbps (offered load of 400pkt/s per station as shown in Table 4)

The obtained measurement results of the successful transmit probabilities of various queueing configurations, along with the calculated successful transmit probability of default FIFO queueing model, are presented in Table 5. The required a_n and b_n values for equal end-to-end throughput as discussed in Section III.B are calculated and shown in the last row of Table 5.

Table 5
The obtained successful transmit probability (a_1, b_1, a_2 and b_2) of the testbed with $1 < C < N$ ($C = 2$) under four different queueing configurations

	a_1	b_1	a_2	b_2
Def (measurement)	0.806	0.823	0.912	0.911
Def (calculated from model)	0.820	0.820	0.912	0.912
L100_M500	0.751	0.835	0.755	0.950
L10_M50	0.757	0.834	0.756	0.950
L10_M40	0.904	0.802	0.906	0.914
Intended a_n and b_n values to equally divide the wireless link capacity (refer to Table 3)	0.760	0.833	0.912	0.912

C. Discussion

From Figure 7, a general traffic graph is shown for the offered load (λ_s) of 400pkt/s. The aggregated mesh traffic at MAP2 is hence 1600pkt/s ($4\lambda_s$). The combination of the aggregated mesh traffic and local offered load ($4\lambda_s + \lambda_s = 2000$pkt/s) at MAP2 exceeded the link capacity ($\mu_{max} = 1824$ pkt/s) and hence can only produce output at the rate of μ_{max}. Similar situation is also experienced by MAP1 ($\mu_{max} + \lambda_s > \mu_{max}$). The successful transmit probability of both the local ingress interfaces (a_1 and a_2) and mesh ingress interfaces (b_1 and b_2) of the congested MAPs (MAP2 and MAP1) can be determined by using Eq. (23) and Eq. (24), respectively. The successful transmit packet rate can then be determined by multiplying the successful transmit probability with the traffic rate. The successful transmit packet rate of the mesh ingress interface at MAP2 is b_2 times $4\lambda_s$.

The end-to-end throughput (λ_{n0}) from the station associated to the local ingress interface of MAP$_n$ can be determined by Eq. (27) (end-to-end throughput of station 2 associated to MAP2 is $\lambda_{20} = b_1 a_2 \lambda_s$).
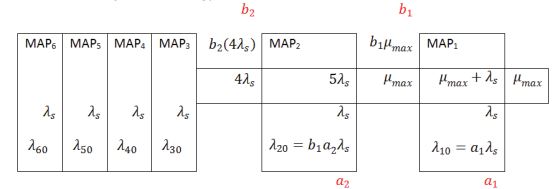

Figure 7: The aggregated offered load at MAP2 ($5\lambda_s$) and MAP1 ($\mu_{max} + \lambda_s$) exceeded the wireless link capacity (μ_{max}) when λ_s is 400pkt/s

From the traffic graph as shown in Figure 8(a) to Figure 8(f), the successful transmit probabilities (a_n and b_n) and end-to-end throughput (λ_{n0}) of different queueing configurations are determined with conditions as previously discussed in Table 3.
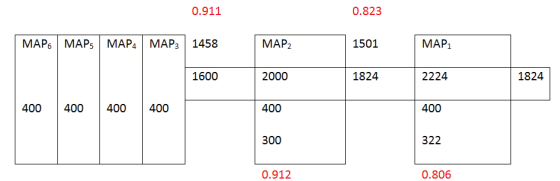

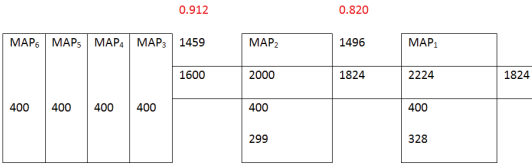Figure 8(a): Traffic graph of Def(measurement)

0.912						0.820	
MAP6	MAP5	MAP4	MAP3	1459	MAP2	1496	MAP1
				1600	2000	1824	2224	1824
400	400	400	400		400		400
					299		328

0.912   0.820

Figure 8(b): Traffic graph of *Def* (calculation)

0.950						0.835	
MAP6	MAP5	MAP4	MAP3	1520	2	1523	1
				1600	2000	1824	2224	1824
400	400	400	400		400		400
					252		300

0.755   0.751
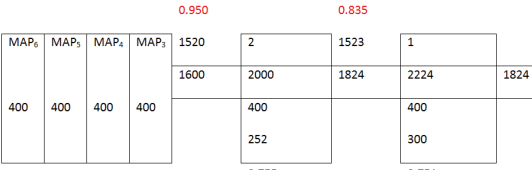
Figure 8(c): Traffic graph of *L100_M500*

0.950						0.834	
MAP6	MAP5	MAP4	MAP3	1520	2	1521	1
				1600	2000	1824	2224	1824
400	400	400	400		400		400
					252		303

0.756   0.757
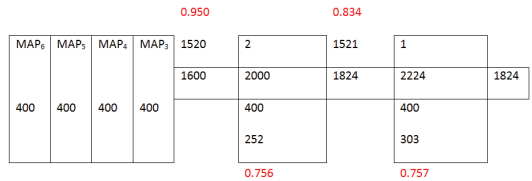
Figure 8(d): Traffic graph of *L10_M50*

0.914						0.802	
MAP6	MAP5	MAP4	MAP3	1462	2	1463	1
				1600	2000	1824	2224	1824
400	400	400	400		400		400
					291		362

0.906   0.904

Figure 8(e): Traffic graph of L10_M40

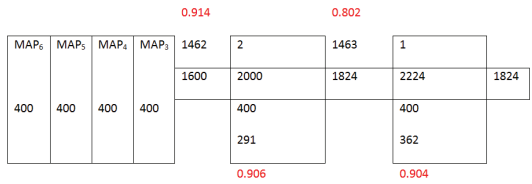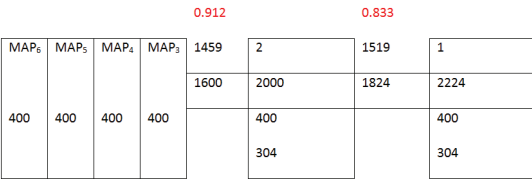| 0.912						0.833	
MAP6	MAP5	MAP4	MAP3	1459	2	1519	1
				1600	2000	1824	2224	18
400	400	400	400		400		400
					304		304

0.912   0.760

Figure 8(f): Traffic graph of intended throughput balancing in Section III.B

For the three queueing configurations other than the *Def*, the increment and decrement of successful transmit probabilities are just the corresponding value in the *Def* used as the reference value. If the packet arrival ratio of local over mesh ingress interface is larger than the respective queue length ratio, the mesh ingress interface successful transmit probability will be higher than the local ingress interface successful transmit probability (such as situations of congested MAPs in *L100_M500* and *L10_M50*). On the other hand, if the packet arrival ratio of local over mesh ingress interface is smaller than the respective queue length ratio, the mesh ingress interface successful transmit probability will be lower than the local ingress interface successful transmit probability

(such as situation of MAP_1 in *L10_M40*). If the packet arrival ratio is equal to the queue length ratio, the mesh successful transmit probability is also equal to the local successful transmit probability (such as situation of MAP_2 in *L10_M40* with error 0.8%). As a conclusion, the hypothesis (Section III.C) which states that "the ratio between the length of local and mesh ingress interface queue can affect the successful transmit probability of the respective interface" is fully validated in this section.

The effect to the end-to-end throughput introduced by the proposed solution is analysed. The hypothesis (Section III.C) "the ratio between the length of local and mesh ingress interface queue can affect the successful transmit probability of the respective interface" is fully validated in Section IV.B. If the packet arrival ratio of local ingress interface over mesh ingress interface is larger than the respective queue length ratio, the mesh ingress interface successful transmit probability will be higher than the local ingress interface successful transmit probability (such as situation of congested MAPs in *L100_M500* and *L10_M50*). On the other hand, if the packet arrival ratio of local ingress interface over mesh ingress interface is smaller than the respective queue length ratio, the mesh ingress interface successful transmit probability will be lower than the local ingress interface successful transmit probability (such as situation of MAP_1 in *L10_M40*). If the packet arrival ratio is equal to the queue length ratio, the mesh successful transmit probability is also equal to the local successful transmit probability (such as situation of MAP_2 in *L10_M40* with 0.8% difference of successful transmit probability).

By controlling the ratio of queue lengths, the spatial bias problem in multi-hop wireless network can be alleviated.

V. CONCLUSION

The root cause of the unbalanced end-to-end throughput problem, equality of local successful transmit probability (a_n) and mesh successful transmit probability (b_n) in congested MAPs introduced by the default queueing manager, is firstly validated at the Introduction section. The differences between successful transmit probabilities are always small (Normal distributed, zero centered for MAP_1. Two modes, major population centered at zero and the second population centered at 0.035 for MAP_2).

Based on the equality of a_n and b_n, an n-hop end-to-end throughput model with deterministic offer load is firstly derived. The required a_n and b_n values to alleviate the unbalanced end-to-end throughput problem is subsequently determined from the model. By configuring the length ratio of both the local and mesh ingress queues in the congested MAPs according to the determined probability (a_n and b_n, respectively), the end-to-end throughput of both MAP_1 and MAP_2 were managed to be suppressed and hence given higher end-to-end throughput to stations further away from the gateway.

VI. FUTURE WORKS

At the moment, the ratio of the queue length is in static condition (e.g. L10_M50). A real-time dynamic way of adjusting the ratio of the queue length shall be implemented to address the actual traffic load.

The side effect of the proposed method was observed as shown in Figure 9. When the total offered load in the wireless network is close to the maximum wireless link capacity ($\sum_{n=1}^{6} \lambda_{n0} \approx \mu_{max}$), the proposed methods (L100_M500 and L10_M50) are experiencing slightly lower end-to-end throughput (5.7% less than Def). The reason behind the side effect shall be studied in the near future.
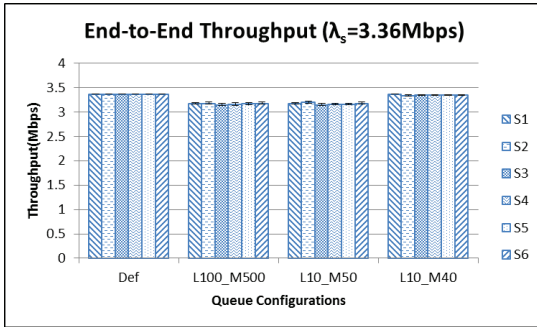

Figure 9: End-to-end throughput result with λ_s = 3.36Mbps (offered load of 300pkt/s per station). The total offered load in the wireless network is close to the maximum wireless link capacity ($\sum_{n=1}^{6}$ 3.36Mbps ≈ 20.46Mbps).

REFERENCES

[1] J. Cardona. (2012). *HOWTO cozybit/open80211s Wiki GitHub*. [Online]. Available: https://github.com/cozybit/open80211s/wiki/HOWTO

[2] S. Avallone, S. Guadagno, D. Emma, A. Pescape, and G. Ventre, "D-ITG distributed internet traffic generator," in *Quantitative Evaluation of Systems, 2004. QEST 2004. Proceedings. First International Conference on the*, 2004, pp. 316-317.

[3] H. Takagi and T. Nishi, "Correlation of interdeparture times in M/G/1 and M/G/1/K queues," *Journal of the Operations Research Society of Japan,* vol. 41, pp. 142-151, 1998.

[4] Y. H. Bae, K. J. Kim, E. Hwang, J. S. Park, and B. D. Choi, "Packet management scheme for location-independent end-to-end delay in IEEE 802.11 s multi-hop wireless mesh networks," in *Telecommunications, 2008. ICT 2008. International Conference on*, 2008, pp. 1-6.

[5] D. Jung, J. Hwang, H. Lim, K.-J. Park, and J. C. Hou, "Adaptive contention control for improving end-to-end throughput performance of multihop wireless networks," *Wireless Communications, IEEE Transactions on,* vol. 9, pp. 696-705, 2010.

[6] R. L. Gomes, W. M. Junior, E. Cerqueira, and A. J. Abelém, "Using fuzzy link cost and dynamic choice of link quality metrics to achieve QoS and QoE in wireless mesh networks," *Journal of Network and Computer Applications,* vol. 34, pp. 506-516, 2011.

[7] B. Pinheiro, V. Nascimento, R. Gomes, E. Cerqueira, and A. Abelem, "A Multimedia-Based Fuzzy Queue-Aware Routing Approach for Wireless Mesh Networks," in *Computer Communications and Networks (ICCCN), 2011 Proceedings of 20th International Conference on*, 2011, pp. 1-7.

[8] M. Fathi, H. Taheri, and M. Mehrjoo, "Cross-layer joint rate control and scheduling for OFDMA wireless mesh networks," *Vehicular Technology, IEEE Transactions on,* vol. 59, pp. 3933-3941, 2010.

[9] D. Nandiraju, L. Santhanam, N. Nandiraju, and D. P. Agrawal, "Achieving load balancing in wireless mesh networks through multiple gateways," in *Mobile Adhoc and Sensor Systems (MASS), 2006 IEEE International Conference on*, 2006, pp. 807-812.

[10] N. S. Nandiraju, D. S. Nandiraju, D. Cavalcanti, and D. P. Agrawal, "A novel queue management mechanism for improving performance of multihop 802.11 s based mesh networks," in *Performance, Computing, and Communications Conference, 2006. IPCCC 2006. 25th IEEE International*, 2006, pp. 7 pp.-168.

[11] N. Chilamkurti and S. A. Prakasam, "Enhanced active queue management for multi-hop networks," *Mobile Networks and Applications,* vol. 16, pp. 771-781, 2011.

[12] C. Lim, C.-H. Choi, and H. Lim, "A weighted RED for alleviating starvation problem in wireless mesh networks," in *Local Computer Networks, 2008. LCN 2008. 33rd IEEE Conference on*, 2008, pp. 841-842.

[13] V. Mancuso, O. Gurewitz, A. Khattab, and E. W. Knightly, "Elastic rate limiting for spatially biased wireless mesh networks," in *INFOCOM, 2010 Proceedings IEEE*, 2010, pp. 1-9.